JACS
JOURNAL OF THE AMERICAN CHEMICAL SOCIETY

Communication

pubs.acs.org/JACS

Dimeric Drug Polymeric Nanoparticles with Exceptionally High Drug Loading and Quantitative Loading Efficiency

Kaimin Cai,[†] Xi He,[†,‡] Ziyuan Song,[†] Qian Yin,[†] Yanfeng Zhang,[†] Fatih M. Uckun,[§,⊥] Chen Jiang,*[,‡] and Jianjun Cheng*[,†]

[†]Department of Materials Science and Engineering, University of Illinois at Urbana—Champaign, Urbana, Illinois 61801, United States

[‡]Key Laboratory of Smart Drug Delivery, Ministry of Education, Department of Pharmaceutics, School of Pharmacy, Fudan University, Shanghai 201203, China

[§]Division of Hematology-Oncology, Systems Immunobiology Laboratory, Children's Center for Cancer and Blood Diseases, Children's Hospital Los Angeles, Los Angeles, California 90027, United States

[⊥]Department of Pediatrics and Norris Comprehensive Cancer Center, University of Southern California, Keck School of Medicine, Los Angeles, California 90027, United States

Supporting Information

ABSTRACT: Encapsulation of small-molecule drugs in hydrophobic polymers or amphiphilic copolymers has been extensively used for preparing polymeric nanoparticles (NPs). The loadings and loading efficiencies of a wide range of drugs in polymeric NPs, however, tend to be very low. In this Communication, we report a strategy to prepare polymeric NPs with exceptionally high drug loading (>50%) and quantitative loading efficiency. Specifically, a dimeric drug conjugate bearing a trigger-responsive domain was designed and used as the core-constructing unit of the NPs. Upon co-precipitation of the dimeric drug and methoxypoly(ethylene glycol)-*block*-polylactide (mPEG-PLA), NPs with a dimeric drug core and a polymer shell were formed. The high-drug-loading NPs showed excellent stability in physiological conditions. No premature drug or prodrug release was observed in PBS solution without triggering, while external triggering led to controlled release of drug in its authentic form.

Polymeric micellar nanoparticles (NPs) are one of the most widely used drug delivery platforms in nanomedicine.[1] This type of NPs contains an internal hydrophobic polymer core and an exterior hydrophilic polymer shell, formed through self-assembly of an amphiphilic copolymer. Hydrophobic drug molecules can be embedded in the micellar hydrophobic cores during the self-assembly process. Although there have been intensive studies on micellar NP-based delivery in the past few decades, clinical success has yet to be realized, due in part to the formulation challenges and intrinsic properties of micelles (e.g., uncontrolled drug release, poor NP stability, etc.) Polymeric micellar NPs usually have very low drug loadings. Drug loadings in most reported micellar systems are lower than 5%; some are even substantially less than 1%.[2] Heterogeneous composition is also major drawback in micelle formulation. Not only do the micelles tend to have broad size distribution, but the formulations often have non-encapsulated drug aggregates, making it very difficult to achieve a safe formulation that can effectively control drug delivery *in vivo*. Undesired drug release from micelles is another critical challenge to overcome.[3] It is very difficult, if not entirely impossible, to control the composition and stability of the formulated polymeric micellar NPs for their clinical applications.[4] In this Communication, we report an unprecedented approach to prepare dimeric drug-encapsulating polymeric NPs that can effectively address the challenges of polymeric nanomedicine mentioned above.

During the self-assembly of drug molecules and amphiphilic copolymers to form the intended drug-encapsulating micelle-like NPs, large drug aggregates often form (Scheme 1a), which significantly lowers the drug loading and loading efficiency in NPs. In the case of hydrophobic drugs that tend to precipitate in aqueous solution, the kinetic process for forming drug aggregates, instead of drug-embedded micelles, may dominate. For example, polymeric micelle formulation with encapsulated camptothecin (CPT),[5] a well-known anticancer agent, yields heterogeneous compositions and very broad particle size distributions (from sub-100 nm to sub-micrometer), presumably due to the fast self-aggregation of CPT molecules because of $\pi-\pi$ interaction of its planar pentacyclic aromatic ring structure that leads to micrometer-size large aggregates (Figure 1a). Moderate encapsulation efficiency and very low drug loading have been reported for CPT polymeric micelles (<5%).[6] To form polymeric NPs with high loading and loading efficiency, we envisioned a new NP structure with the amphiphilic polymers acting as surface stabilizers while the drug molecules constitute the bulk structure in the NPs. We hypothesize that inhibiting the fast kinetics of drug aggregation may lead to drug aggregates small enough to be used as the core to form high-drug-loaded NPs upon interaction with amphiphilic copolymers.

To prevent formation of large drug aggregates/crystals in the formulation (Scheme 1a), one approach is to introduce "structural defects" to the drug/prodrug molecules and make the drug molecules structurally less rigid so that their packing efficiency is reduced, preventing long-range order of drug

Received: December 22, 2014
Published: March 5, 2015

DOI: 10.1021/ja513034e
J. Am. Chem. Soc. 2015, 137, 3458−3461

Scheme 1. Schematic Illustration of Encapsulating Hydrophobic Drugs into Nanoparticles[a]

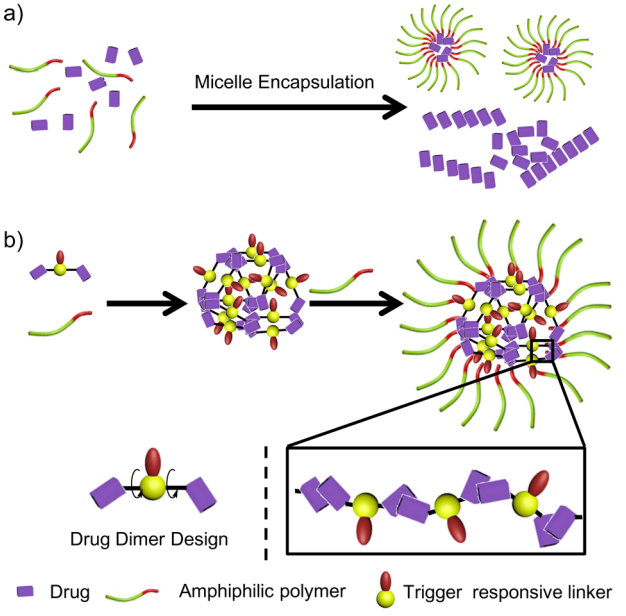

[a](a) Hydrophobic drugs are encapsulated in a polymeric micelle with undesired formation of large drug precipitates. (b) Illustration of drug dimer nano-aggregation followed by surface coating and particle stabilization by an amphiphilic polymer via hydrophobic interaction.

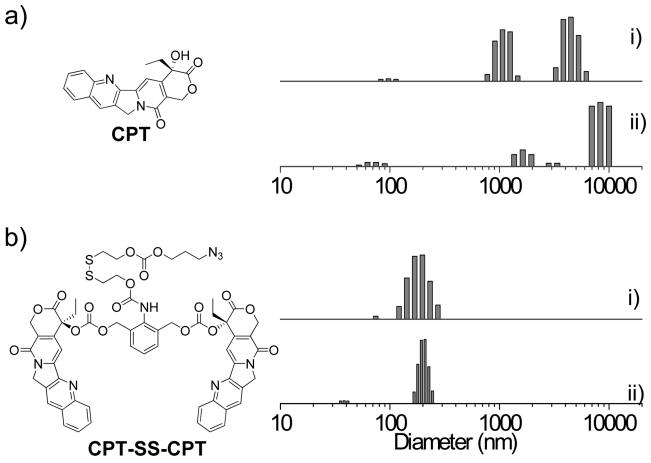

Figure 1. (a) Chemical structure of camptothecin (CPT) and size distribution of CPT/mPEG-PLA NPs formulated through nano-precipitation at CPT/mPEG-PLA weight ratios of 1:1 (i) and 1:10 (ii). (b) Chemical structure of CPT-SS-CPT and size distribution of CPT-SS-CPT/mPEG-PLA NPs formulated through nano-precipitation at CPT-SS-CPT/mPEG-PLA weight ratios of 1:1 (i) and 10:1 (ii).

packing. One such specific approach is to covalently link drug dimers with σ bonds that can freely rotate (Scheme 1b). We hypothesize that this drug dimer design can substantially inhibit long-range-ordered drug molecule packing and therefore prevent formation of large particles. In addition, compared to free drug, dimeric prodrug should have increased intermolecular hydrophobic interactions because of increased surface area and an augmented tendency for prodrug aggregation due to the freely rotatable σ bonds that can position the drug molecule at any desired angle for intermolecular drug interaction (Scheme 1b), which leads to core cross-linking and improved NP stability. In addition, when the linkage in the dimeric drug conjugate is cleaved to give two single drugs in the aggregates, the drug molecules would be much less stably packed and more prone to dissociate (be released) from the aggregates. Therefore, such dimeric drug design can potentially result in particles with much lower prodrug release tendency until the dimeric drug is cleaved to a single drug, minimizing undesired drug release during formulation and post-formulation processes, which is a key challenge for drug encapsulation. If the drug dimers could self-aggregate to certain sizes (<200 nm, typical size of nanomedicine) before stabilization of the particle surfaces by amphiphilic copolymers, exceptionally high drug loading and quantitative loading efficiency would be expected.

We used CPT as a model drug to validate our design. We first precipitated CPT from DMF to water without addition of amphiphilic copolymers. CPT precipitates were formed instantaneously upon addition of water to the CPT/DMF solution (Supporting Information, Figure S2). When CPT was co-precipitated with mPEG-PLA at 1:1 (w/w) ratio, micrometer-size particles (precipitates) and multiple distributions were observed (Table 1, entry 1, and Figure 1a(i)). When the amount of CPT was reduced by 10 times to a CPT/mPEG-PLA ratio of 0.1 (w/w) (Table 1, entry 2), there was no substantial change in the heterogeneity of the formulation; multimodal dynamic light scattering (DLS) peaks depicted the co-existence of sub-100 nm polymeric micelles and micrometer-size drug aggregates (Figure 1a(ii)). Thus, CPT/mPEG-PLA NPs prepared via nano-precipitation follow the typical micellation and drug aggregation process as shown in Scheme 1a.

Table 1. Formulation of CPT, CPT-SS-CPT, and Dox-SS-Dox with mPEG-PLA via Nanoprecipitation in DMF−H_2O[a]

entry	drug	ratio (w/w) drug/mPEG-PLA	d (nm)	LE (%)[b]	DL (%)[c]
1	CPT	1.0	2669[d]		
2	CPT	0.1	4588[d]		
3	CPT-SS-CPT	1.0	171	>99	29
4	CPT-SS-CPT	4.0	174	>99	46
5	CPT-SS-CPT	6.0	165	>99	49
6	CPT-SS-CPT	10.0	181	>99	52
7	Dox-SS-Dox	4.0	221	88	53

[a]100 μL of a DMF solution of drug/mPEG-PLA was added dropwise into 2.0 mL of deionized water. [b]Drug loading efficiency, defined as the ratio of the amount of drug in the nanoparticle to the total amount of drug applied in formulation of the nanoparticles. [c]Drug loading of CPT/Dox, defined as the weight ratio of drug to nanoparticles. [d]Large aggregates were observed.

To validate the dimer design strategy for preparing high loading NPs, we designed and synthesized a dimeric CPT derivative, CPT-SS-CPT (Figure 1b). To modulate drug release from the drug/polymer NP, we designed such CPT conjugates in which CPT molecules are stably conjugated to the dimers via carbonate linkages that are subject to triggered bond cleavage and subsequent drug release by a reducing reagent.[7] Specifically, two CPT molecules are conjugated to 2,6-bis(hydroxymethyl)-aniline (BHA)[7] through carbonate linkages in CPT-SS-CPT. The amine group of the aniline is protected by a disulfide bond bearing a flexible chain. Upon triggering, cleavage of the disulfide bond in CPT-SS-CPT would result in decomposition of the drug

DOI: 10.1021/ja513034e
J. Am. Chem. Soc. 2015, 137, 3458−3461

dimer, releasing CPT in its authentic form (Scheme S4). CPT-SS-CPT has much lower water solubility (less than 10 ng/mL) than CPT (3 μg/mL),[8] presumably due to stronger intermolecular interactions between CPT-SS-CPT molecules (illustrated in Scheme 1b). We compared CPT-SS-CPT with CPT in the same formulation experiments as described above. The CPT-SS-CPT was first precipitated from DMF to water. As expected, CPT-SS-CPT formed much smaller aggregates than CPT (Figure S2). When a mixture of CPT-SS-CPT and mPEG-PLA (1:1, w/w) was precipitated in water, DLS analysis showed monomodal distribution, indicating homogeneous NP formation (Figure 1b(i)). No precipitation was observed during formulation; the loading efficiency was determined to be quantitative (Table 1, entry 3). This formulation gave a dimeric drug conjugate loading as high as 50% (corresponding to 29% CPT equivalent loading). We also attempted to use a mixture of CPT-SS-CPT/mPEG-PLA at a weight ratio up to 10:1 for making CPT-SS-CPT/mPEG-PLA NP (SS NPs) (Table 1, entries 4–6; Table S1). In all cases, sub-200 nm NPs with monomodal DLS distribution were obtained, suggesting homogeneous formulation and well-controlled composition (see representative trace of CPT-SS-CPT/mPEG-PLA (10:1, w/w) NP, Figure 1b(ii)). The NPs are stable in phosphated buffer saline (PBS) and human serum for at least 3 days (Figure S3) with no size change observed. Notably, the formulated NPs remained stable at concentrations well below the critical micelle concentration (CMC) of the mPEG-PLA (Figure S4a,b), indicating non-dynamic NP structures irrespective of micelles and substantiating the suggested mode of dimeric drug interaction (Scheme 1b). As a comparison, a "monomeric" CPT derivative, CPT-SS, linking CPT directly to the disulfide side chain without the aniline fragment (structure see Scheme S2) resulted in an uncontrolled large aggregate when it was co-precipitated with mPEG-PLA at a 1:1 drug/polymer ratio (Table S1, entry 10). The results further demonstrate the necessity of the dimer structure for high loading formation: dimeric structure affords stronger intermolecular drug interactions than both CPT and CPT-SS.

We next designed experiments to further study the NP formulation. When a DMF solution of CPT-SS-CPT (in the absence of mPEG-PLA) was dropwise added to water, the CPT-SS-CPT aggregates grew larger over time, reaching ~6 μm at t = 60 min (denoted as rectangle, Figure 2a). When CPT-SS-CPT was added to water followed by the addition of mPEG-PLA 10 and 30 s later, particle size was stabilized at 850 and 1100 nm, respectively (denoted as triangle and circle, Figure 2a), suggesting the successful coating of CPT-SS-CPT aggregates with mPEG-PLA. When mPEG-PLA empty micelles (without CPT-SS-CPT) were pre-formed (~50 nm) followed by the addition of a DMF solution of CPT-SS-CPT (1/16 relative to mPEG-PLA, w/w) (illustrated in Figure 2b), drug-loaded NPs with size around 180 nm (monomodal DLS peak, Figure S5) were formed, with complete disappearance of the 50 nm distribution (Figure 2c). Mixing CPT-SS-CPT with pre-formed mPEG-PLA micelles clearly modulates the original mPEG-PLA micellar structure, as the size of the NPs increased dramatically. Further addition of CPT-SS-CPT solutions did not change the average size of the NPs (Figure 2c). TEM analysis revealed a core–shell nanostructure (Figures 2d and S6), suggesting rapid formation of CPT-SS-CPT nanoaggregate that recruited mPEG-PLA to stabilize it through the hydrophobic interaction of hydrophobic drug core and the hydrophobic PLA segment.

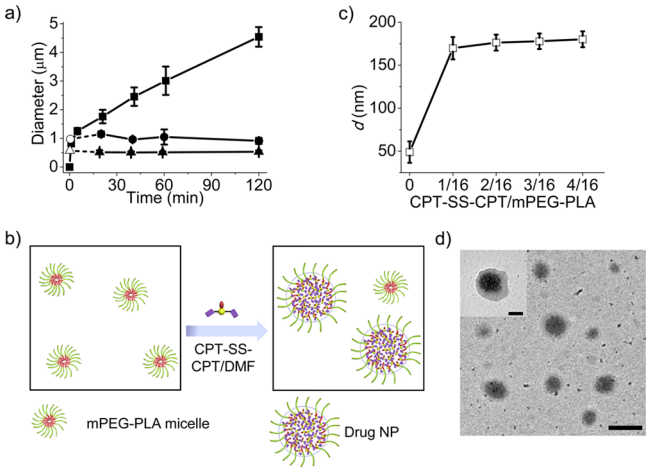

Figure 2. (a) CPT-SS-CPT nanoaggregate size change as a function of time without mPEG-PLA (■) and with mPEG-PLA, 10 s (▲) and 30 s (●) after water dilution. (b) Schematic illustration of post-addition experiment. DMF solution of CPT-SS-CPT was added into aqueous solution of mPEG-PLA micelle. (c) Size change of mPEG-PLA micelles after the addition of CPT-SS-CPT solution. Data are presented as mean value ± standard deviation of four independent measurements. (d) TEM image of NP prepared in (c). Scale bar = 400 nm. Inset: Enlarged view of the NP. Scale bar = 50 nm.

An important feature of the drug dimer design is its trigger-responsive property due to the stable carbonate linkage and cleavable side chain. We next evaluated the release profile of SS NPs by model thiol triggers. Considering the elevated level of thiol species in a variety of cells,[9] the SS NPs would preferentially release active CPT intracellularly instead of a burst release during blood circulation. Authentic CPT release from SS NPs was measured by co-incubation with dithiothreitol (DTT). The SS NPs showed controlled release over 48 h, while negligible CPT release was detected in the absence of DTT (Figure 3b), and only the free drug was detected over the course of the study (Figure 3a). Thus, this is a very rare example of drug-encapsulating NPs (drugs not covalently bound to polymer matrices) with complete elimination of the burst release effect, due presumably to the drug dimer "cross-linking" as illustrated in Scheme 1b.

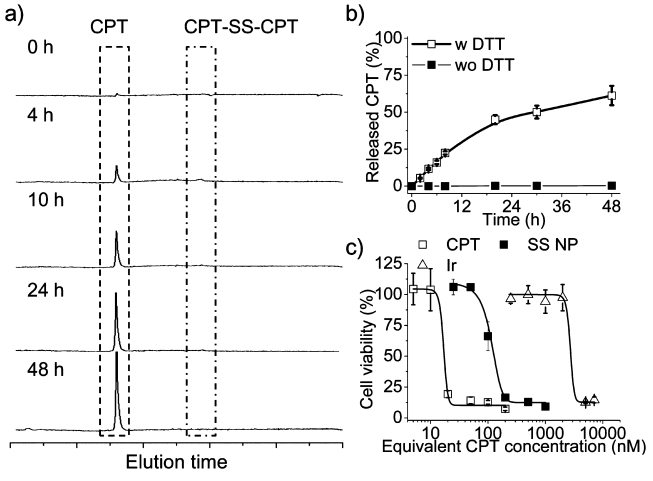

Figure 3. (a) HPLC analysis of CPT release from the SS NPs in the presence of 10 mM DTT as thiol trigger. (b) CPT release from SS NPs with/without thiol trigger (DTT) in PBS. (c) Cytotoxicity of the SS NPs in HeLa cells.

DOI: 10.1021/ja513034e
J. Am. Chem. Soc. 2015, 137, 3458–3461

The anticancer effect of the SS NPs was then evaluated *in vitro* by MTT assay. By incubating HeLa cells with the SS NPs for 72 h, significant cell proliferation inhibition was observed in a drug/NP concentration-dependent manner (Figure 3c). The IC_{50} of the SS NPs was 114 nM, compared to 17 nM for free CPT. Irinotecan (Ir), a clinically used CPT derivative, had an IC_{50} value of 2700 nM under the same conditions. The significant cytotoxicity of the high-loading NPs indicated the intracellular thiols actively reduced the disulfide bond within the NPs, releasing CPT in a timely manner.

We next tested whether this strategy can be used for nano-formulation of other drugs with strong crystallization tendency, such as doxorubicin (Dox). Dox-SS-Dox was synthesized, sharing the same trigger-responsive linker as CPT-SS-CPT (structure see Scheme S3). When Dox-SS-Dox/mPEG-PLA at a ratio of 4/1 (w/w) was precipitated, NPs with size of 221 nm and monomodal DLS distribution were obtained (Table 1, entry 7). The loading efficiency was determined to be 88%, and the equivalent doxorubicin loading was calculated to be 53%. Compared with the conventional micelle[10] and liposome encapsulation[11] method, this dimeric drug strategy greatly improved the drug loading and loading efficiency of the Dox in NPs.

In summary, we found that simply dimerizing drug and using the drug dimer for encapsulation with amphiphilic polymer can drastically improve drug loading and NP properties. Drug can be encapsulated in polymer NPs with over 50% drug loading and close to 100% loading efficiency. Unlike direct encapsulation of free drugs in polymer micelles that have drug burst release and micelle stability issues, this drug−dimer conjugate encapsulating NP showed excellent stability and completely eliminated the burst release effect. This NP formulation strategy provides a new and likely scalable[12] route to encapsulate hydrophobic drugs efficiently without complicated carrier polymer design and screening. We are investigating whether this strategy can be broadly applied to nano-formulation of drugs other than CPT and Dox and how the size can be controlled below 100 nm.[13]

■ ASSOCIATED CONTENT

Supporting Information

Experimental procedures, stability of the NPs, TEM images of the NPs, CMC measurement of the mPEG-PLA, and characterization of new compounds. This material is available free of charge via the Internet at http://pubs.acs.org.

■ AUTHOR INFORMATION

Corresponding Authors

*jiangchen@shmu.edu.cn
*jianjunc@illinois.edu

Notes

The authors declare no competing financial interest.

■ ACKNOWLEDGMENTS

This work was supported by the National Science Foundation (Career Program DMR-0748834 and DMR-1309525) and the National Institutes of Health (NIH Director's New Innovator Award 1DP2OD007246-01 (J.C.), 1R21CA152627 (J.C.), U01-CA-151837 (F.M.U.) and R01-CA-154471 (F.M.U.)). K.C. and Q.Y. were supported by NIH National Cancer Institute Alliance for Nanotechnology in Cancer 'Midwest Cancer Nanotechnology Training Center' Grant R25 CA154015A. X.H. was supported by China Scholarship Council as a visiting student.

■ REFERENCES

(1) (a) Ma, L.; Kohli, M.; Smith, A. *ACS Nano* **2013**, *7*, 9518−9525. (b) Yang, Y.; Pearson, R. M.; Lee, O.; Lee, C. W.; Chatterton, R. T.; Khan, S. A.; Hong, S. *Adv. Funct. Mater.* **2014**, *24*, 2442−2449. (c) Petros, R. A.; DeSimone, J. M. *Nat. Rev. Drug Discov.* **2010**, *9*, 615−627.

(2) (a) Matsumura, Y. *Adv. Drug Deliv. Rev.* **2008**, *60*, 899−914. (b) Chen, K. J.; Tang, L.; Garcia, M. A.; Wang, H.; Lu, H.; Lin, W. Y.; Hou, S.; Yin, Q.; Shen, C. K.; Cheng, J.; Tseng, H. R. *Biomaterials* **2012**, *33*, 1162−1169. (c) Cheng, J.; Teply, B. A.; Sherifi, I.; Sung, J.; Luther, G.; Gu, F. X.; Levy-Nissenbaum, E.; Radovic-Moreno, A. F.; Langer, R.; Farokhzad, O. C. *Biomaterials* **2007**, *28*, 869−876. (d) Xu, J.; Zhao, Q.; Jin, Y.; Qju, L. *Nanomedicine* **2014**, *10*, 349−358.

(3) (a) Bromberg, L. *J. Controlled Release* **2008**, *128*, 99−112. (b) Attia, A. B. E.; Ong, Z. Y.; Hedrick, J. L.; Lee, P. P.; Ee, P. L. R.; Hammond, P. T.; Yang, Y. Y. *Curr. Opin. Colloid Interface Sci.* **2011**, *16*, 182−194. (c) Wei, H.; Volpatti, L. R.; Sellers, D. L.; Maris, D. O.; Andrews, I. W.; Hemphill, A. S.; Chan, L. W.; Chu, D. S.; Horner, P. J.; Pun, S. H. *Angew. Chem., Int. Ed.* **2013**, *52*, 5377−5381. (d) Zhang, L.; Sinclair, A.; Cao, Z.; Ella-Menye, J. R.; Xu, X.; Carr, L. R.; Pun, S. H.; Jiang, S. *Small* **2013**, *9*, 3439−3444. (e) Wang, Y.; Byrne, J. D.; Napier, M. E.; DeSimone, J. M. *Adv. Drug Deliv. Rev.* **2012**, *64*, 1021−1030.

(4) (a) Wang, J.; Sun, X.; Mao, W.; Sun, W.; Tang, J.; Sui, M.; Shen, Y.; Gu, Z. *Adv. Mater.* **2013**, *25*, 3670−3676. (b) Shen, Y.; Jin, E.; Zhang, B.; Murphy, C. J.; Sui, M.; Zhao, J.; Wang, J.; Tang, J.; Fan, M.; Van Kirk, E.; Murdoch, W. J. *J. Am. Chem. Soc.* **2010**, *132*, 4259−4265. (c) Peer, D.; Karp, J. M.; Hong, S.; FarokHzad, O. C.; Margalit, R.; Langer, R. *Nat. Nanotechnol.* **2007**, *2*, 751−760. (d) Gao, W. W.; Vecchio, D.; Li, J. M.; Zhu, J. Y.; Zhang, Q. Z.; Fu, V.; Li, J. Y.; Thamphiwatana, S.; Lu, D. N.; Zhang, L. F. *ACS Nano* **2014**, *8*, 2900−2907. (e) Pornpattananangkul, D.; Zhang, L.; Olson, S.; Aryal, S.; Obonyo, M.; Vecchio, K.; Huang, C. M.; Zhang, L. F. *J. Am. Chem. Soc.* **2011**, *133*, 4132−4139.

(5) (a) Herben, V. M.; Ten Bokkel Huinink, W. W.; Schellens, J. H.; Beijnen, J. H. *Pharm. World Sci.* **1998**, *20*, 161−172. (b) Pommier, Y. *Nat. Rev. Cancer* **2006**, *6*, 789−802. (c) Pommier, Y. *ACS Chem. Biol.* **2013**, *8*, 82−95.

(6) (a) Min, K. H.; Park, K.; Kim, Y. S.; Bae, S. M.; Lee, S.; Jo, H. G.; Park, R. W.; Kim, I. S.; Jeong, S. Y.; Kim, K.; Kwon, I. C. *J. Controlled Release* **2008**, *127*, 208−218. (b) Liu, J.; Jiang, Z.; Zhang, S.; Saltzman, W. M. *Biomaterials* **2009**, *30*, 5707−5719. (c) Choi, K. Y.; Yoon, H. Y.; Kim, J. H.; Bae, S. M.; Park, R. W.; Kang, Y. M.; Kim, I. S.; Kwon, I. C.; Choi, K.; Jeong, S. Y.; Kim, K.; Park, J. H. *ACS Nano* **2011**, *5*, 8591−8599. (d) Luo, Y. L.; Yang, X. L.; Xu, F.; Chen, Y. S.; Zhang, B. *Colloids Surf. B: Biointerfaces* **2014**, *114*, 150−157. (e) Ueki, K.; Onishi, H.; Sasatsu, M.; Machida, Y. *Drug Dev. Res.* **2009**, *70*, 512−519. (f) Zhang, L.; Hu, Y.; Jiang, X.; Yang, C.; Lu, W.; Yang, Y. H. *J. Controlled Release* **2004**, *96*, 135−148.

(7) (a) Zhang, Y.; Yin, Q.; Yin, L.; Ma, L.; Tang, L.; Cheng, J. *Angew. Chem., Int. Ed.* **2013**, *52*, 6435−6439. (b) Zhang, Y.; Ma, L.; Deng, X.; Cheng, J. *Polym. Chem.* **2013**, *4*, 224−228.

(8) Stella, V. J.; Nti-Addae, K. W. *Adv. Drug Deliv. Rev.* **2007**, *59*, 677−694.

(9) Lee, M. H.; Yang, Z.; Lim, C. W.; Lee, Y. H.; Dongbang, S.; Kang, C.; Kim, J. S. *Chem. Rev.* **2013**, *113*, 5071−5109.

(10) (a) Yoo, H. S.; Lee, K. H.; Oh, J. E.; Park, T. G. *J. Controlled Release* **2000**, *68*, 419−431. (b) Yoo, H. S.; Oh, J. E.; Lee, K. H.; Park, T. G. *Pharm. Res.* **1999**, *16*, 1114−1118.

(11) Eloy, J. O.; Claro de Souza, M.; Petrilli, R.; Barcellos, J. P.; Lee, R. J.; Marchetti, J. M. *Colloids Surf. B: Biointerfaces* **2014**, *123*, 345−363.

(12) (a) Rietscher, R.; Thum, C.; Lehr, C. M.; Schneider, M. *Pharm. Res.* **2014**, DOI: 10.1007/s11095-014-1612-z. (b) Galindo-Rodriguez, S. A.; Puel, F.; Briancon, S.; Allemann, E.; Doelker, E.; Fessi, H. *Eur. J. Pharm. Sci.* **2005**, *25*, 357−367.

(13) Tang, L.; Yang, X.; Yin, Q.; Cai, K.; Wang, H.; Chaudhury, I.; Yao, C.; Zhou, Q.; Kwon, M.; Hartman, J. A.; Dobrucki, I. T.; Dobrucki, L. W.; Borst, L. B.; Lezmi, S.; Helferich, W. G.; Ferguson, A. L.; Fan, T. M.; Cheng, J. *Proc. Natl. Acad. Sci. U.S.A.* **2014**, *111*, 15344−15349.

DOI: 10.1021/ja513034e
J. Am. Chem. Soc. 2015, 137, 3458−3461